

Detonations and deflagrations in cosmological phase transitions

Ariel Mégevand* and Alejandro D. Sánchez†

IFIMAR (CONICET-UNMdP),

Departamento de Física, Facultad de Ciencias Exactas y Naturales, UNMdP,

Deán Funes 3350, (7600) Mar del Plata, Argentina

Abstract

We study the steady state motion of bubble walls in cosmological phase transitions. Taking into account the boundary and continuity conditions for the fluid variables, we calculate numerically the wall velocity as a function of the nucleation temperature, the latent heat, and a friction parameter. We determine regions in the space of these parameters in which detonations and/or deflagrations are allowed. In order to apply the results to a physical case, we calculate these quantities in a specific model, which consists of an extension of the Standard Model with singlet scalar fields. We also obtain analytic approximations for the wall velocity, both in the case of deflagrations and of detonations.

1 Introduction

Phase transitions of the universe may give rise to a variety of cosmological relics, such as the baryon asymmetry of the universe [1], cosmic magnetic fields [2], topological defects [3], inhomogeneities [4], and gravitational waves [5, 6, 7]. To be observable, several of these relics depend on the strength of the phase transition. In a first-order phase transition, bubbles of the stable phase nucleate and grow inside the supercooled phase. The expansion of bubbles provides a departure from thermal equilibrium, which is generally required to generate cosmological remnants. The mechanisms of relic generation depend in general on the motion of the bubble walls (either because they are based on charge transport near the bubble walls, on the collisions of the walls, or on the turbulence they produce). As a consequence, an important parameter in the generating mechanisms is the velocity of bubble expansion. For some relics, higher velocities give a stronger effect. This is the case, e.g., of gravitational waves. In other cases, on the contrary, the amplitude or abundance of the relic peaks at some value of the bubble wall velocity. This happens for instance in the case of electroweak baryogenesis.

*Member of CONICET, Argentina. E-mail address: megevand@mdp.edu.ar

†Member of CONICET, Argentina. E-mail address: sanchez@mdp.edu.ar

A first-order phase transition requires the system to have two phases with different equation of state (EOS), which coexist in some temperature range. Thus, the high-temperature phase has a pressure $p_+(T)$, and the low-temperature phase has a pressure $p_-(T)$. At the critical temperature T_c , the two phases have the same pressure but different entropy and energy. The entropy density is given by $s(T) = p'(T)$, where a prime denotes derivation with respect to T , and the energy density is given by $\rho(T) = Ts(T) - p(T)$. The latent heat L is defined as the difference between the energy densities of the two phases at $T = T_c$. Therefore, we have $p_+(T_c) = p_-(T_c)$ and $L = T_c(p'_+(T_c) - p'_-(T_c))$. Furthermore, all these quantities can be derived from the free energy density \mathcal{F} by the relation $p(T) = -\mathcal{F}(T)$.

In a finite temperature field theory, we have in general a scalar field ϕ , the Higgs field, which plays the role of an order parameter for the phase transition. We shall assume this is the case, although most of our conclusions will be independent of this assumption. The free energy density is the finite temperature effective potential, which is a function of ϕ and T . In some range of temperatures, the free energy has two minima separated by a barrier. The value of ϕ in each minimum defines the two phases. We shall assume that the high-temperature minimum is $\phi = 0$, and the low temperature minimum has a value $\phi_m(T) \neq 0$, which is the case for a symmetry breaking phase transition. A phase transition with a large value of the order parameter, $\phi_m(T) > T$ is usually called a strongly first-order phase transition. Thus, we have $\mathcal{F}_+(T) = \mathcal{F}(0, T)$ and $\mathcal{F}_-(T) = \mathcal{F}(\phi_m(T), T)$. Below the critical temperature, the transition from $\phi = 0$ to $\phi = \phi_m(T)$ occurs via the nucleation of bubbles [8, 9]. A bubble is a configuration $\phi(x)$ of the field. We shall make the usual assumption that this configuration is a thin-walled sphere. A nucleated bubble grows because $p_-(T) > p_+(T)$ for $T < T_c$.

The propagation of bubble walls in cosmological phase transitions has been extensively investigated [10, 11, 12, 13, 14, 15, 16, 17, 18, 19, 20, 21, 22, 23, 24, 25]. In general, the stronger the phase transition, the larger the amount of supercooling. Therefore, one expects that the velocity of bubble walls will be larger for stronger phase transitions. Indeed, the pressure difference which pushes the wall of a bubble, $\Delta p(T) = p_-(T) - p_+(T)$, grows as the temperature decreases. On the other hand, the velocity depends also on the friction of the wall with the medium and the latent heat that is released at the phase transition front. The friction is related to the *microphysics*, i.e., to the interactions of particles of the medium with the Higgs field in the configuration of the wall, whereas the latent heat is involved in the *hydrodynamics*, i.e., the bulk motions and reheating of the fluid near the wall.

According to hydrodynamics, there are two kinds of steady state solutions for the propagation of the wall, namely, detonations and deflagrations. Detonations are supersonic while deflagrations are generally subsonic. Each solution has different boundary conditions, and both may appear in a given model and may even coexist in some range of parameters. A numerical calculation of the evolution of the field $\phi(x, t)$ [10], suggests that the bubbles grow typically as subsonic deflagrations, although, in some regions of parameter space, the solutions switch from deflagrations to detonations, as the friction is decreased. In view of the cosmological consequences of the phase transition, it is important to determine the range of parameters where each solution may exist. Hydrodynamic considerations give general constraints on the allowed regions of thermodynamic param-

eters, but the existence of deflagrations and detonations depends strongly on the value of the friction.

The literature on the subject of the bubble wall velocity can be roughly divided in two groups: those papers which calculate the friction for a given model, assuming nonrelativistic deflagrations and ignoring hydrodynamics [11, 12, 13, 14, 15, 16, 17], and those which consider hydrodynamics, but they either disregard microphysics or include the friction as a free parameter [10, 18, 19, 20, 21, 22, 23, 24]. As a consequence, the analytical approximations that are most commonly used in applications, were derived ignoring either microphysics or hydrodynamics. Indeed, in the context of baryogenesis the wall velocity is assumed to be of the form $v_w \approx \Delta p(T)/\eta$, where η is a friction coefficient. This is a nonrelativistic approximation (thus appropriate for the case of deflagrations) which neglects hydrodynamics. In the context of gravitational waves, on the contrary, the wall is assumed to propagate as a detonation, and the so called Chapman-Jouguet hypothesis is further assumed, leading to a simple expression for the velocity, which depends only on the ratio between the latent heat and the thermal energy density of the plasma.

The aim of this paper is to calculate the wall velocity in both cases, detonations and deflagrations, taking the friction into account. This will allow us to investigate under which conditions the various hydrodynamic solutions can exist, and to explore how these conditions are attained in a physical model. For these purposes, we shall first consider the equations for the discontinuity of the fluid variables across the wall, together with a simple parametrization of the friction force (which consists in introducing a damping term in the equation for the field ϕ) and a simple model (the bag equation of state) for the phase transition. These simplifications permit to write down a complete set of equations, which can be solved for the wall velocity as a function of three parameters, namely, $\alpha_c = L/(4\tilde{\rho}_+(T_c))$, where L is the latent heat and $\tilde{\rho}_+(T)$ is the thermal energy density of the high-temperature phase, $\alpha_N = L/(4\tilde{\rho}_+(T_N))$, where $T_N < T_c$ is the temperature at which bubbles nucleate, and η/L , where η is the friction coefficient.

Solving numerically these equations, we shall determine the regions in the space of the aforementioned parameters for which deflagrations and detonations may or may not exist. In order to apply the results to a physical model, we choose as an example the electroweak phase transition in an extension of the Standard Model (SM) with scalar singlets, which provides a simple variation of the strength of the phase transition as a function of the fundamental parameters. For this specific model, we compute the quantities α_c , α_N , and η/L and we calculate the wall velocity. To estimate the value of the parameter η , we shall relate our parametrization of the friction to the microphysics calculations that exist in the literature. For the nucleation temperature T_N , we solve numerically the bounce action to obtain the nucleation rate. We shall also find analytical approximations for both propagation modes. In particular, we give a simple approximation for the detonation solution, which depends on the friction.

The paper is organized as follows. In section 2 we write down the equations for the wall velocity, the fluid variables, and the friction for both propagation modes. In section 3 we show the numerical results for the wall velocity as a function of the relevant parameters, and we determine regions in parameter space where each kind of solution may or may not exist. In section 4 we consider a specific model, for which we compute the values of the latent heat L , the friction η , and the nucleation temperature T_N , and we calculate the

detonation and deflagration velocities (when they exist) as functions of the fundamental parameters of the model. Finally, in section 5 we consider analytical approximations for the wall velocity. Our conclusions are summarized in section 6.

2 The wall velocity

To take into account hydrodynamics and microphysics in the calculation of the wall velocity, three basic ingredients are needed, namely, the continuity conditions that relate the fluid variables across the wall discontinuity, an equation of state, which relates the various fluid variables on each side of the phase transition front, and an equation for the effect of friction on the motion of the wall.

2.1 Hydrodynamics

In the rest frame of the phase-transition front, we have an incoming flow in the high-temperature phase, with velocity v_+ , and an outgoing flow in the low-temperature phase, with velocity v_- (see Fig. 1). The motion of the wall causes the temperatures T_+ and T_- on each side to be different. The continuity conditions for energy and momentum fluxes give two equations [26],

$$w_+ \gamma_+^2 v_+ = w_- \gamma_-^2 v_-, \quad w_+ \gamma_+^2 v_+^2 + p_+ = w_- \gamma_-^2 v_-^2 + p_-, \quad (1)$$

where $\gamma = 1/\sqrt{1-v^2}$ and $w = \rho + p = Ts$ is the enthalpy density. Equivalently, we have

$$v_+ v_- = \frac{(p_+ - p_-)}{(\rho_+ - \rho_-)}, \quad \frac{v_+}{v_-} = \frac{(\rho_- + p_+)}{(\rho_+ + p_-)}, \quad (2)$$

which can be readily solved for the velocities in terms of the thermodynamical quantities. Notice that these two equations have four unknowns, namely, the velocities v_{\pm} and the temperatures T_{\pm} on both sides of the wall. All other thermodynamical quantities are determined by the equation of state. In principle, the temperature T_+ of the supercooled phase can be calculated using the nucleation rate. To determine completely the system, one more equation is needed. This can be obtained from a microscopic calculation of the friction of the wall with the plasma.

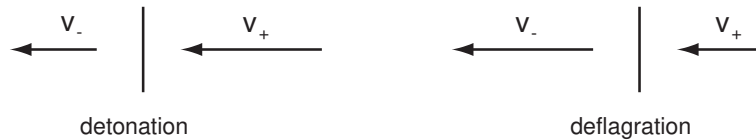


Figure 1: The velocities on each side of the wall, in the reference frame of the wall.

The above equations admit two kinds of solutions, one of them with $|v_-| < |v_+|$, called detonation, and the other with $|v_-| > |v_+|$, called deflagration (Fig. 1). This can be seen by using a simple model in which the low-temperature EOS is that of radiation,

$p_- = \rho_-/3$, and the high-temperature EOS is that of radiation plus vacuum energy, i.e., $\rho_+ = \tilde{\rho}_+ + \varepsilon$, with $p_+ = \tilde{\rho}_+/3 - \varepsilon$. From Eqs. (1) or (2) one obtains [18]

$$v_+ = \frac{\frac{1}{6v_-} + \frac{v_-}{2} \pm \sqrt{\left(\frac{1}{6v_-} + \frac{v_-}{2}\right)^2 + \alpha^2 + \frac{2}{3}\alpha - \frac{1}{3}}}{1 + \alpha}, \quad (3)$$

where $\alpha = \varepsilon/\tilde{\rho}_+$. The solutions with the plus and the minus signs correspond to detonations and to deflagrations, respectively. We plot both in Fig. 2 for a given value of α . It turns out that, for a detonation, we have $|v_+| > c_{s+}$, and for a deflagration, $|v_+| < c_{s+}$, where $c_{s\pm}$ is the speed of sound on each side of the wall. For the above simple equations of state, the speed of sound in both phases is that of a relativistic plasma, $c_{s\pm} = (dp_{\pm}/d\rho_{\pm})^{1/2} = 1/\sqrt{3}$.

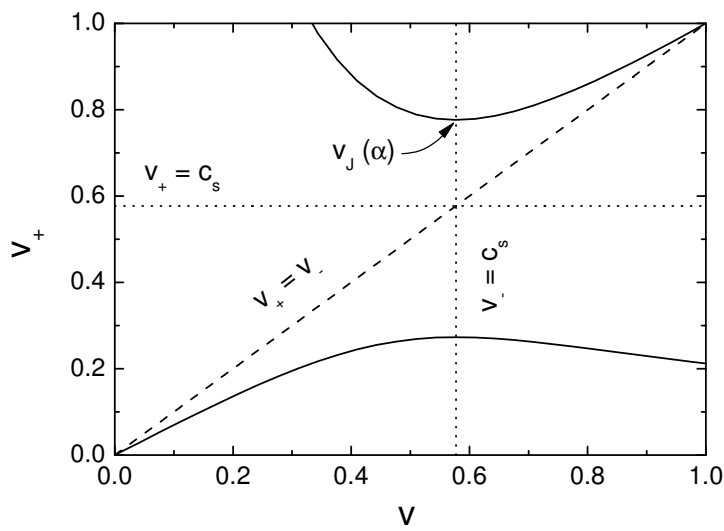


Figure 2: v_+ vs v_- according to Eq. (3), for $\alpha = 0.1$

In the reference frame where the matter far in front of the bubble wall is at rest and the wall moves, the matter at the center of the bubble (far behind the wall) must be also at rest. As a consequence, a single front (the phase transition front) is not sufficient to satisfy all the boundary conditions. As a result, it turns out that a deflagration front must be preceded by a shock front (Fig. 3, left). Between the shock and the deflagration fronts, the matter is compressed and has a finite velocity. Outside this region the matter is at rest. On the other hand, a detonation front hits fluid which is at rest, the density increases suddenly, and the phase transition front is followed by a rarefaction wave (Fig. 3, right). Comparing with the reference frame of the wall, we see that the deflagration wall velocity is given by $v_w = |v_-|$, while the detonation wall velocity is given by $v_w = |v_+|$. According to the inequalities above, a detonation is always supersonic, $v_w > c_{s+}$. A deflagration may in principle be supersonic or subsonic (it *is* subsonic with respect to the fluid in front of it, which is moving in the direction of the wall).

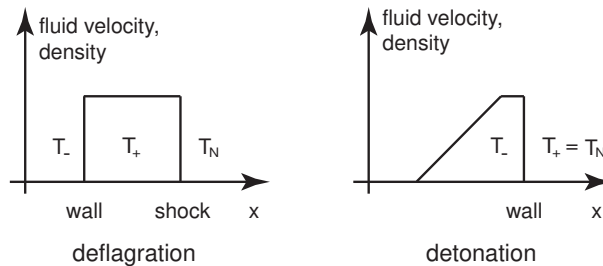


Figure 3: Schematically, the profile of the density or the velocity of the fluid, induced by the moving wall.

2.1.1 Strong and weak solutions

Depending on the velocity v_- of the outflow, deflagrations are divided into weak ($|v_-| < c_{s-}$), Jouguet ($|v_-| = c_{s-}$) and strong ($|v_-| > c_{s-}$) deflagrations. Thus, strong deflagrations are supersonic, and weak deflagrations are subsonic. Detonations are also classified into strong ($|v_-| < c_{s-}$), Jouguet ($|v_-| = c_{s-}$), and weak ($|v_-| > c_{s-}$) detonations. Since the incoming flow is supersonic, strong detonations perturb the fluid more strongly than weak detonations.

The various kinds of solutions have been extensively investigated [10, 18, 19, 20, 21]. Using thermodynamical arguments, one can find regions in parameter space where each solution is allowed. In particular, the non-negativity of entropy production may rule out the whole family of detonations or deflagrations [21]. However, such arguments do not rule out a particular type (i.e., weak, Jouguet, or strong) of detonation or deflagration [22]. In the case of deflagrations, in Ref. [22] it is argued that strong deflagrations are mechanically unstable, although in principle there is no physical reason against their existence. A special type of supersonic Jouguet deflagration, which is followed by a rarefaction wave, was shown to exist in Ref. [23].

In the case of detonations, it is known [26] that, for the case of chemical burning, detonation bubbles can only grow as Jouguet detonations. Remarkably, this condition (which is referred to as the Chapman-Jouguet hypothesis) means that a microscopic calculation of the wall velocity is irrelevant, since the system is completely determined by the energy-momentum conservation and the boundary conditions. In Ref. [18] it was argued that the Chapman-Jouguet hypothesis should be valid also for cosmological phase transitions. Setting $v_- = c_s$ in Eq. (3) leads to a very simple formula $v_w = v_J(\alpha)$ for the wall velocity. However, it was shown in Ref. [22] that, in contrast to the case of chemical burning, the Chapman-Jouguet hypothesis does not hold in the case of phase transitions. It was also shown in Refs. [18, 22] that strong detonations are impossible, since they cannot satisfy the boundary condition of a vanishing fluid velocity at some point behind the bubble wall. Nevertheless, weak detonations are possible, and the velocity will be determined in general by microscopical processes. Thus, in a realistic model the detonation velocity will depend on a friction parameter η as well as on the hydrodynamic parameter α . The wall velocity will always satisfy the condition $v_w(\alpha, \eta) \geq v_J(\alpha)$ (as can be seen in Fig. 2). Hence, v_w may give the Jouguet result only in some limiting cases.

2.1.2 Detonations vs deflagrations

It is well known that, if the supercooling is not considerable and the friction is large enough, the bubbles will grow as deflagrations, whereas detonations demand small values of the friction and more extreme conditions (i.e., strong supercooling) [10, 19, 21]. It is often argued, though, that the propagation of the deflagration wall becomes turbulent and eventually turns into a detonation due to shape instabilities of the wall. As discussed in Ref. [27] for the case of the QCD phase transition and in Ref. [28] for the case of the electroweak phase transition, small wavelength perturbations of the deflagration front are stabilized by the interface tension, while large ones grow exponentially. However, a more detailed study [29] shows that the strong dependence of the wall velocity on temperature actually stabilizes the large scale perturbations. The stability of the deflagration front thus depends on several quantities (these are essentially the latent heat, the value of the wall velocity and its dependence on temperature). It was found, in particular, that the deflagration front is stable under perturbations *at all scales* for velocities above a certain critical value v_c . For instance, in the (unrealistic) case of the minimal Standard Model with a Higgs mass $m_H = 40\text{GeV}$, the critical velocity is $v_c \approx 0.07$ [29]. Below this velocity, perturbations are unstable on scales larger than a critical scale λ_c . However, depending on the parameters, the value of λ_c may be much larger than the size of bubbles. Furthermore, the characteristic time for the growth of the instabilities may be larger than the duration of the phase transition. Therefore, in the general case, the deflagration front will be probably stable. A study of the hydrodynamical stability of bubble growth is beyond the scope of this paper.

2.2 Microphysics

In any case, it is clear that the determination of the wall velocity requires additional input. To consider the effect of friction together with the fluid equations (1), it is customary to introduce a damping term of the typical form $u^\mu \partial_\mu \phi$ in the equation of motion for the Higgs field [10],

$$\partial_\mu \partial^\mu \phi + \frac{\partial \mathcal{F}(\phi, T)}{\partial \phi} + (T_c \tilde{\eta}) u^\mu \partial_\mu \phi = 0. \quad (4)$$

Here, the dimensionless damping coefficient $\tilde{\eta}$ is a free parameter. Nevertheless, we can relate $\tilde{\eta}$ to the actual friction coefficient obtained from microscopical calculations in a specific model, as we shall see in section 4.4.1. For simplicity, we shall consider a planar wall moving along the z axis. In the frame of the wall we have

$$-\phi'' + \partial \mathcal{F} / \partial \phi + T_c \tilde{\eta} u \phi' = 0, \quad (5)$$

where $u = \gamma v$, with v the fluid velocity in the z direction.

Multiplying by $\phi'(z)$ and integrating over $-\infty < z < +\infty$, the first term disappears. Then, *if we neglect the variation of temperature with z* , the fluid velocity is $v = -v_w$, and we obtain

$$\mathcal{F}(0, T) - \mathcal{F}(\phi_m, T) = T_c \tilde{\eta} \sigma \gamma v_w, \quad (6)$$

where

$$\sigma = \int [\phi'(z)]^2 dz \quad (7)$$

is the surface tension of the bubble wall. Equation (6) gives the well known nonrelativistic approximation for the wall velocity

$$v_w \approx \Delta\mathcal{F}(T)/\eta, \quad (8)$$

where

$$\eta = \tilde{\eta}T_c\sigma, \quad (9)$$

and $\Delta\mathcal{F}$ is the free energy density difference $\mathcal{F}_+(T) - \mathcal{F}_-(T)$, which gives the pressure difference $\Delta p = p_-(T) - p_+(T)$ between the two phases.

If we now take into account hydrodynamics, we can still integrate Eq. (5), but we cannot ignore the fact that the temperature and velocity of the fluid depend on z . Before multiplying by ϕ' and integrating, we use the equation $\partial\mathcal{F}/\partial\phi = d\mathcal{F}/d\phi - (\partial\mathcal{F}/\partial T)(\partial T/\partial\phi)$ [10]. Then, proceeding as before, we obtain

$$\mathcal{F}(0, T_+) - \mathcal{F}(\phi_m(T_-), T_-) - \int_{T_-}^{T_+} \frac{\partial\mathcal{F}}{\partial T} dT + \tilde{\eta}T_c \int_{-\infty}^{+\infty} [\phi'(z)]^2 u(z) dz = 0. \quad (10)$$

The first two terms are just $\mathcal{F}_+(T_+) - \mathcal{F}_-(T_-) = p_- - p_+$. To simplify the calculations, some approximations are necessary. In the first integral, the function $\partial\mathcal{F}/\partial T(\phi(x), T(x))$ varies from

$$\frac{\partial\mathcal{F}}{\partial T}(\phi_m(T_-), T_-) = \frac{d\mathcal{F}_-}{dT}(T_-) = -s_-(T_-) \quad (11)$$

to

$$\frac{\partial\mathcal{F}}{\partial T}(0, T_+) = \frac{d\mathcal{F}_+}{dT}(T_+) = -s_+(T_+) \quad (12)$$

(we have used the fact that ϕ_m and 0 are minima of \mathcal{F}). If $\phi(x)$ and $T(x)$ change smoothly, we expect that a linear function will give a good approximation to the integrand $\partial\mathcal{F}/\partial T$ inside the thin wall. Therefore, the integral yields $-(s_- + s_+)(T_+ - T_-)/2$. For the second integral, it is a good approximation to assume that ϕ'^2 is symmetric around the center of the wall at $z = 0$; hence, this can be approximated by $\sigma(u_+ + u_-)/2$ [10]. Hence, we have

$$p_+ - p_- - \frac{1}{2}(s_+ + s_-)(T_+ - T_-) + \frac{\eta}{2}(v_+\gamma_+ + v_-\gamma_-) = 0, \quad (13)$$

where $\eta = \tilde{\eta}T_c\sigma$ as before.

Notice that the approximations we have made to obtain Eq. (13) do not involve any assumption on the wall velocity nor on the equation of state. Hence, this equation can be used for the treatment of relativistic as well as nonrelativistic velocities, and is model-independent. Provided the various thermodynamical quantities are related by means of an equation of state, Eqs. (1) and (13) can be solved to obtain the velocities v_- and v_+ as functions of the temperature T_+ in front of the wall. The result will depend on parameters of the theory that appear in the EOS, such as the latent heat, and on the friction coefficient. In practice, however, it is very difficult to solve these equations unless we use a simple model.

2.3 The equation of state

As we have seen, the relation (3) between v_+ and v_- can be derived from Eqs. (1), using the relations

$$p_- = \rho_-/3 \quad (14)$$

for the low-T phase, and

$$\rho_+ = \tilde{\rho}_+ + \varepsilon, \quad p_+ = \tilde{\rho}_+/3 - \varepsilon \quad (15)$$

for the high-T phase. In order to obtain a second relation between v_+ and v_- from Eq. (13), the EOS for each phase has to be more specific. The *thermal* energy densities $\rho_-(T)$ and $\tilde{\rho}_+(T)$ must be of the form aT^4 , where $a = \pi^2 g/30$ and g is the number of relativistic degrees of freedom. Hence, the simplest possibility is to assume that both phases have the same a . Such a simple model was considered in Ref. [18]. This model, however, fails to describe a realistic phase transition if the vacuum energy ε is a constant. Indeed, the critical temperature is defined as that T at which the pressures of the two phases are equal, $p_+(T_c) - p_-(T_c) = 0$. However, with $p_+ = aT^4/3 - \varepsilon$ and $p_- = aT^4/3$, we have $p_+(T) - p_-(T) = -\varepsilon$ at any T . This would be possible if ε were a function of T . With ε constant, this model does not have a critical temperature.

The existence of a critical temperature T_c , below which bubbles nucleate and grow, constitutes an important distinction between the case of a phase transition and that of chemical burning. In a phase transition, supercooling is needed for bubbles to grow. In the first place, the temperature must *decrease sufficiently* below T_c so that bubbles nucleate. In the second place, even if for some reason (e.g., by means of inhomogeneous nucleation) bubbles nucleate at $T = T_c$, the condition $T < T_c$ is still necessary to achieve a pressure difference $p_-(T) > p_+(T)$, so that bubbles can grow. In the case of chemical burning, the speed of the reaction increases with temperature, and the temperature must *rise sufficiently* for the combustion to proceed. If the reaction is strongly exothermic, it is sufficient to rise the temperature at a single point. The heat that is released by the reaction at that point rises the temperature of the surrounding gas, and the reaction may extend over the whole gas [26]. As a consequence, the higher the released energy, the larger the velocity of the combustion front. In the case of a phase transition, the release of latent heat is not necessary for the process to continue. On the contrary, the reheating of the supercooled gas *slows down* the phase transition, as the temperature approaches T_c .¹

To keep the EOS as simple as possible, we shall consider ε constant, and different values a_+ and a_- in the two phases. This gives the well known bag equation of state, which is appropriate to a system with a first-order phase transition:

$$\begin{aligned} \rho_+ &= a_+ T^4 + \varepsilon, & p_+ &= a_+ T^4/3 - \varepsilon, \\ \rho_- &= a_- T^4, & p_- &= a_- T^4/3, \end{aligned} \quad (16)$$

and the entropy is given by $s_{\pm} = \frac{4}{3} a_{\pm} T^3$. Since Eq. (3) was derived using the relations (14,15), the result is still valid as a function of $\alpha = \varepsilon/\tilde{\rho}_+$, with $\tilde{\rho}_+ = a_+ T_+^4$. However,

¹The process we have just described corresponds to a deflagration or slow combustion. For the detonation case one can argue similarly. Essentially, in the case of chemical burning, the combustion takes place behind the detonation front because the temperature is risen by the front. Evidently, a phase transition does not need such a temperature rise.

the parameter ε has a different meaning in each model. Indeed, with $a_+ = a_-$ the energy released in the phase transition is just ε . In a realistic model the vacuum energy ε does not coincide with the latent heat $L = \rho_+(T_c) - \rho_-(T_c)$, since entropy is released together with vacuum energy. For the bag equation of state, the critical temperature is readily obtained by equating the pressures p_+ and p_- . We have

$$(a_+ - a_-) T_c^4 = 3\varepsilon, \quad (17)$$

from which we obtain the latent heat

$$L = 4\varepsilon. \quad (18)$$

In fact, in a realistic model, the vacuum energy density does not vanish immediately after the phase transition. Hence, we will have in general two parameters ε_{\pm} , one for each phase. Nevertheless, this only amounts to replacing $\varepsilon = \varepsilon_+ - \varepsilon_-$ in Eqs. (17,18) and in the definition of α . The expression of α in terms of the latent heat, $\alpha = L/(4\tilde{\rho}_+)$, remains unchanged. For simplicity, we shall set $\varepsilon_- = 0$ in the following.

Notice that the positivity of the pressure at $T = T_c$ (i.e., $p_+ = p_- > 0$) implies that the ratio

$$\alpha_c \equiv \varepsilon / (a_+ T_c^4) \quad (19)$$

cannot be arbitrarily large, namely, $\alpha_c < 1/3$. This relation between the vacuum and the thermal energy densities is valid beyond this simple model [30].

Using the fluid conditions (1) and the equations of state (16), the friction equation (13) becomes

$$\frac{p_+ - p_-}{\tilde{\rho}_+} - \frac{2}{3} \left(1 + \frac{s_-}{s_+}\right) \left(1 - \frac{T_-}{T_+}\right) + \frac{2\alpha_+ \eta}{L} (|v_+| \gamma_+ + |v_-| \gamma_-) = 0, \quad (20)$$

with

$$\frac{p_+ - p_-}{\tilde{\rho}_+} = \alpha_+ \frac{4v_+ v_-}{1 - 3v_+ v_-}, \quad (21)$$

$$\frac{s_-}{s_+} = \frac{a_-}{a_+} \left(\frac{T_-}{T_+}\right)^3, \quad \frac{T_-}{T_+} = \left(\frac{a_+ \rho_-}{a_- \tilde{\rho}_+}\right)^{1/4}, \quad (22)$$

and

$$\frac{\rho_-}{\tilde{\rho}_+} = 1 - \alpha_+ \frac{1 + v_+ v_-}{1/3 - v_+ v_-}, \quad (23)$$

where we have used instead of α the notation

$$\alpha_+ \equiv \varepsilon / (a_+ T_c^4). \quad (24)$$

The velocities are further related by Eq. (3), with the + sign for detonations and the - sign for deflagrations, and the ratio a_-/a_+ is a parameter of the model. Using Eqs. (17) and (19) we can write

$$a_-/a_+ = 1 - 3\alpha_c. \quad (25)$$

It can be seen from Eqs. (2) that $v_+ v_- \leq 1/3$. Hence, according to Eq. (21), we have $p_+(T_+) - p_-(T_-) > 0$. This means that the temperature difference that is established around the wall inverts *locally* the relation $p_-(T) > p_+(T)$, which holds for $T < T_c$.

We can solve the above equations for v_+ or v_- as a function of T_+ (or, equivalently, α_+) and the parameters η and α_c . In the case of detonations, the temperature T_+ in front of the bubble wall is just the temperature T_N at which bubbles nucleate, so we have

$$\alpha_+ = \alpha_N \equiv \frac{\varepsilon}{a_+ T_N^4} \quad (\text{detonations}), \quad (26)$$

and the fluid on that side of the wall is at rest, so

$$v_w = |v_+|. \quad (27)$$

Thus, we only need to solve Eqs. (20-23) to obtain v_w . This makes this case in general simpler than the deflagration case².

In the case of deflagrations, we must relate the temperature T_+ of the fluid in the reheated region between the phase-transition front and the shock front, to the nucleation temperature T_N of the fluid beyond the shock front (see Fig. 3). To do that, we must consider the fluid conditions (1) for the shock front discontinuity. These are simpler than those for the wall, since we have the same phase on both sides of this front. Calling v_1 the velocity of the fluid in front of the shock and v_2 the velocity behind it, we have, in the reference frame of the shock front [26],

$$|v_1| = \frac{1}{\sqrt{3}} \left(\frac{3T_+^4 + T_N^4}{3T_N^4 + T_+^4} \right)^{1/2}, \quad |v_2| = \frac{1}{3|v_1|}. \quad (28)$$

In the ‘‘laboratory’’ frame, the fluid is at rest behind the phase transition discontinuity, and also ahead of the shock front, so we have

$$v_w = |v_-|, \quad (29)$$

whereas v_1 gives the velocity of the shock front, $v_1 = -v_{\text{sh}}$. The velocity of the fluid v_{fl} between the two fronts can be computed from the velocities v_+ and v_- , or from v_1 and v_2 . Equating both results we find the relation between T_+ and T_N ,

$$\frac{\sqrt{3}(\alpha_N - \alpha_+)}{\sqrt{(3\alpha_N + \alpha_+)(3\alpha_+ + \alpha_N)}} = \frac{v_+ - v_-}{1 - v_+ v_-} \quad (\text{deflagrations}). \quad (30)$$

Thus, we can find $v_w(\alpha_c, \alpha_N, \eta)$, both in the case of a detonation and of a deflagration. Notice that the parameter α_c gives the ratio of latent heat to thermal energy density at $T = T_c$. Thus, for α_c fixed, the parameter α_N gives a measure of the amount of supercooling, since $\alpha_N/\alpha_c = (T_c/T_N)^4$. We have seen that $0 < \alpha_c < 1/3$. On the other hand, α_N is only bounded below, $\alpha_N > \alpha_c$. Nevertheless, in general we will have $T_N \sim T_c$ and $\alpha_N \lesssim 1$. We could have $\alpha_N \gg \alpha_c$ only in a phase transition with extremely strong supercooling.

²If we wanted to find the temperature or velocity profiles inside the bubble, then we would have to consider the equations for the fluid behind the wall and impose boundary conditions at the center of the bubble.

3 Numerical results

We have solved numerically Eqs. (20-23) and (3), with Eqs. (26,27) for detonations and Eqs. (29,30) in the case of deflagrations. In this section we present the numerical results, considering independent variations of the parameters α_c , α_N and η . Nevertheless, we shall make variations around two reference sets of parameters, corresponding to different points in the physical model of section 4 (indicated by crosses in Fig. 11). We choose $\alpha_c \approx 1.27 \times 10^{-2}$, $\alpha_N \approx 1.48 \times 10^{-2}$, $\eta/L \approx 4.03 \times 10^{-2}$, which are obtained when the fundamental parameters of the model are such that the phase transition is rather strongly first-order, i.e., the order parameter is $\phi_N/T_N \approx 2$; and $\alpha_c \approx 3.19 \times 10^{-3}$, $\alpha_N \approx 3.25 \times 10^{-3}$, $\eta/L \approx 2.48 \times 10^{-2}$, obtained from a weaker phase transition, but still with $\phi_N/T_N \approx 1$.

3.1 Detonations

Let us consider a strong phase transition ($\phi_N/T_N \approx 2$). In Fig. 4 (left panel), we have fixed the values of α_c and η/L , and we have varied α_N , starting from $\alpha_N = \alpha_c$, i.e., we have decreased the supercooling temperature T_N below T_c . For α_N close to α_c , no detonation

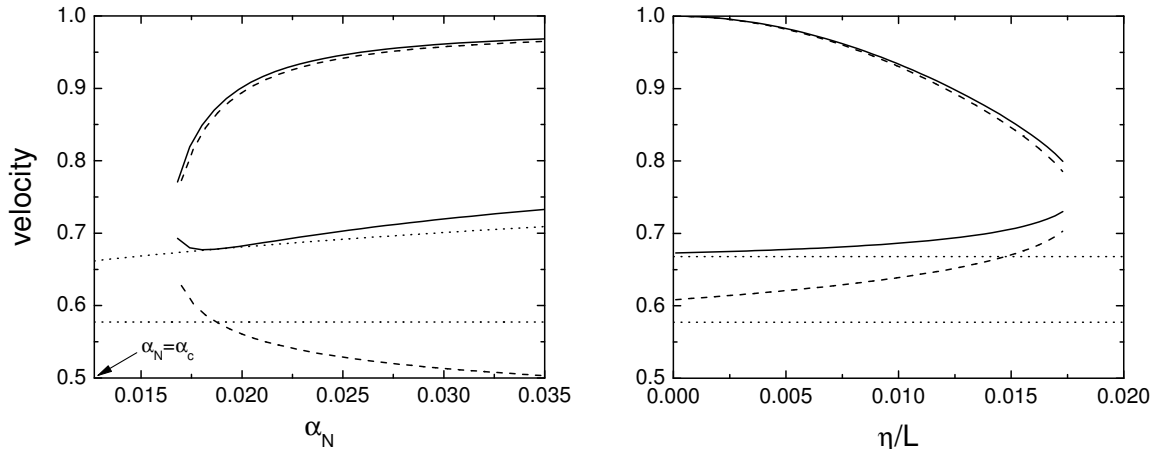


Figure 4: Detonation solutions for $\alpha_c \approx 1.27 \times 10^{-2}$. Left: the velocities as functions of α_N for $\eta/L \approx 4.03 \times 10^{-2}$. Right: the velocities as functions of η/L for $\alpha_N \approx 1.48 \times 10^{-2}$. Solid lines indicate the velocity v_w of the wall, dashed lines the velocity v_- of the outgoing fluid, and dotted lines the speed of sound (lower curves) and the Jouguet velocity (upper curves).

solutions exist (i.e., some supercooling is required). When α_N is large enough we find two solutions for the detonation wall velocity (solid lines). One of them (lower solid curve) is close to the Jouguet velocity $v_J(\alpha_N)$, which is indicated by the upper dotted line. This solution, however, does not seem to be physical. In the first place, the velocity *decreases with the supercooling* until it reaches the Jouguet point. Beyond this point, the velocity increases, but the solution has become a strong detonation, since the velocity v_- (lower dashed curve) crosses below the speed of sound (indicated by the lower dotted line). The other solution, in contrast, is always a weak detonation (the corresponding velocity v_- is indicated by the upper dashed curve). As a matter of fact, this detonation is quite weak,

as the outflow velocity v_- is very close to the inflow velocity $v_+ = v_w$, which implies that the fluid is almost unperturbed by the wall.

This behavior can also be seen if we fix α_c and α_N , and plot the wall velocity as a function of η (Fig. 4, right panel). If the friction is strong enough, no detonation solution exists. For lower values of the friction parameter, we have two solutions, but the lower branch corresponds to a velocity which decreases as the friction is decreased. Depending on the values of the parameters, this solution eventually becomes a strong detonation for low values of η . In any case, as can be seen in the figure, the lower branch solution is much stronger than that of the upper branch. For these reasons, we shall discard this solution.

3.2 Deflagrations

Solving numerically Eqs. (20-23), (3), and (30), we find again two solutions. However, one of them must be discarded, since it has a wrong behavior as a function of the parameters: the velocity decreases with the supercooling and increases with the friction, and is in general supersonic. The correct solution, on the other hand, goes to zero for small supercooling and strong friction. As an illustration, we plot both solutions in Fig. 5 for the case of a strong phase transition, as functions of α_N and η . In contrast to the detonation case, the deflagration solution always exists in the limit of small supercooling, $\alpha_N \rightarrow \alpha_c$. On the other hand, the deflagration solution may not exist when the supercooling becomes too strong or when the friction becomes too low, as this example illustrates.

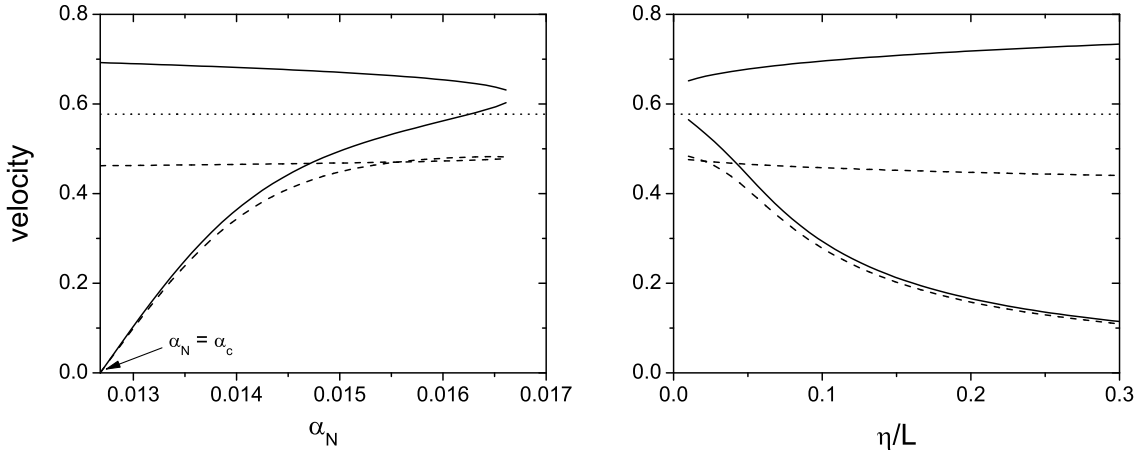


Figure 5: Deflagration solutions for the same case as Fig. 4. Solid lines indicate the velocity v_w of the wall, dashed lines the velocity v_+ of the incoming fluid, and dotted lines the speed of sound.

In the high supercooling and low friction range, we have the detonation solution. We have plotted the physical detonations and deflagrations together in Fig. 6. Solid lines correspond to the case of Figs. 4 and 5, and dashed lines correspond to variation of parameters beginning from a weaker phase transition (with $\phi_N/T_N \approx 1$). As can be seen in the right panel, for α_c and α_N fixed, a stronger phase transition gives, for the same

friction, a larger velocity (solid line). On the contrary, if we vary α_N (left panel), the solid line gives lower velocities. This is because in this plot we are considering the the same amount of supercooling for the two models. Therefore, the model with a larger value of α_c (i.e., of L) gives a lower velocity. Indeed, a larger L causes a larger reheating, thus slowing down the phase transition (both in the deflagration and in the detonation case).

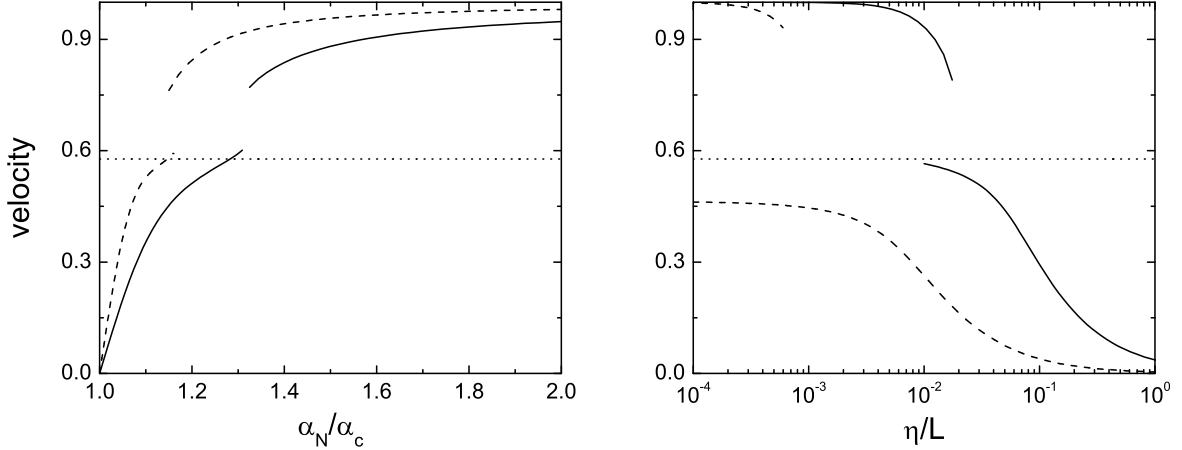


Figure 6: Deflagration and detonation solutions as functions of α_N (left) and of η/L (right) for two families of phase transitions.

In Fig. 6 we see that different situations may arise as the parameters are varied. There are ranges in which detonations and deflagrations coexist, and there are values of α_N and η for which neither solution exists. Fixing α_c , we have calculated the maximum friction for which detonations exist, and the minimum friction that permits the existence of deflagrations. We have plotted these limiting values in Fig. 7 (solid and dashed lines, respectively). Since the curves cross, the plane is divided into four regions, in which there exist either deflagrations, detonations, both, or none. In the latter case, no stationary state of bubble expansion is reached. In the case in which both solutions exist, which of them is realized will depend on the initial conditions and on the stability of each solution. Figure 8 shows the four regions for different values of α_c .

It is difficult to determine in general which of these situations may arise in a physical case. For that aim we would need some relation between the parameters η/L , α_N , and α_c . In the next section we explore the physical case by considering a particular model, for which we calculate the relevant parameters η , L , and T_N as functions of the fundamental parameters of the model. Nevertheless, some general conclusions can be drawn from Fig. 7. Notice that the key parameter for the existence of detonations is the supercooling parameter α_N/α_c : even for $\eta = 0$, detonations exist only if α_N/α_c is large enough. On the contrary, deflagrations exist up to a certain amount of supercooling, even for $\eta = 0$. Therefore, in a phase transition with small supercooling, we will have only deflagrations, no matter how small the friction may be. This is because hydrodynamics brakes the propagation of the wall, thus acting effectively as a friction. This can also be seen in Fig. 8, by the fact that, as we increase α_c (i.e., L), the deflagration region grows and the detonation region reduces.

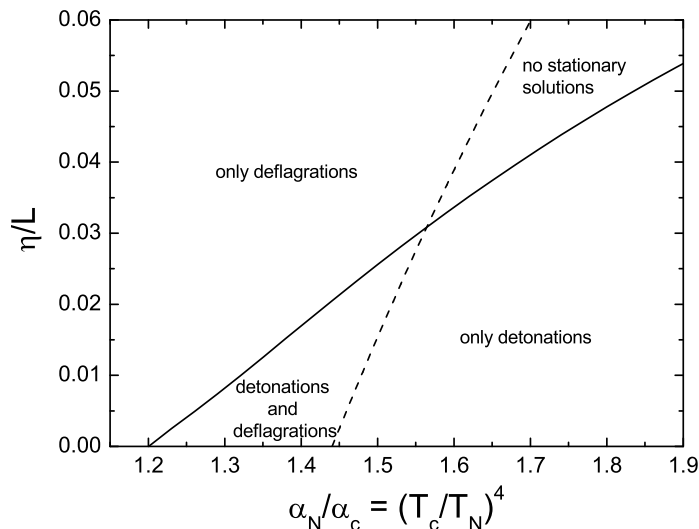


Figure 7: The regions of the parameters η and α_N , for $\alpha_c = 0.05$, where detonations and deflagrations exist. Solid line: maximum friction for detonations. Dashed line: minimum friction for deflagrations.

Observing Figs. 7 or 8 we see that, setting $\eta = 0$ we find, for each α_c , the minimum α_N for which detonations *may* exist and the minimum value for which deflagrations *may* not exist. Besides, the value at which the detonation and deflagration curves cross defines the minimum α_N for which there could be no solution. Fig. 9 shows these three values of α_N as functions of α_c . These curves divide the (α_c, α_N) plane in four regions. In the lower region, detonations do not exist, independently of the value of η ; in the next region detonations will exist if the value of η is small enough; in the third region, deflagrations will not exist if η is too small; in the upper region, neither solution will exist in a certain range of the friction parameter. Deflagrations always exist in the two lower regions and, for large enough friction, in all the (α_c, α_N) plane.

4 The wall velocity in a physical model

So far we have calculated the wall velocity as a function of the latent heat L , the supercooling temperature T_N , and the friction coefficient η . In a physical model these quantities are not independent. However, the simple EOS (16) does not allow to calculate T_N nor η . We shall now consider a model which permits to obtain these quantities as functions of a single fundamental parameter. The model we seek should be as simple as possible, and allow for phase transitions of different strength as the parameters are varied. It is well known that the electroweak phase transition is only a smooth crossover in the minimal Standard Model (SM), whereas many extensions of the model give a strongly first-order phase transition. Therefore, we choose the simplest extension of the SM, namely, adding to the model a gauge singlet scalar S with zero vacuum expectation value [31, 32, 33]. Besides the coupling to the Higgs, which is of the form $2h^2 S^\dagger S H^\dagger H$, the field S may have a mass term $\mu^2 S^\dagger S$ and a quartic term $\lambda_S (S^\dagger S)^2$. We will ignore the possibility

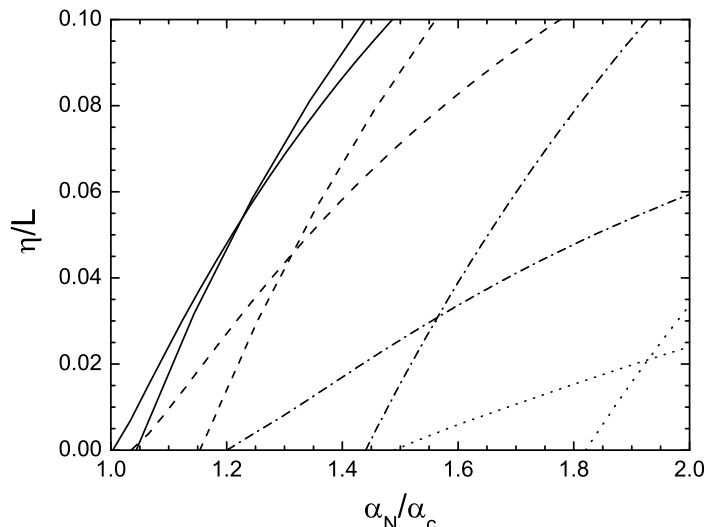


Figure 8: The four regions in the plane (α_N, η) (as in figure 7) for $\alpha_c = 10^{-3}$ (solid), 10^{-2} (dashed), 5×10^{-2} (dashed-dotted), and 10^{-1} (dotted).

that cubic terms exist in the tree-level potential, which may produce a barrier between minima at $T = 0$. Recently, an extension of the SM with several real singlets S_i has been considered [34]. These bosons constitute a hidden sector which couples only to the SM Higgs doublet through a term $h^2 H^\dagger H \sum S_i^2$. If the fields S_i do not have mass terms, so that they only get a mass from electroweak breaking, the phase transition can be made exceedingly strong.

4.1 The effective potential

Our model will consist of a scalar field ϕ (the background Higgs field, $\langle H^0 \rangle \equiv \phi/\sqrt{2}$) with tree-level potential

$$V_0(\phi) = -m^2\phi^2 + \frac{\lambda}{4}\phi^4, \quad (31)$$

for which the vacuum expectation value of the Higgs is given by $v = \sqrt{2/\lambda}m = 246\text{GeV}$, and λ fixes the Higgs mass, $m_H^2 = 2\lambda v^2$. Imposing the renormalization conditions that the minimum of the potential and the mass of ϕ do not change with respect to their tree-level values [33], the one-loop zero-temperature correction is given by

$$V_1(\phi) = \sum_i \frac{\pm g_i}{64\pi^2} \left[m_i^4(\phi) \left(\log \left(\frac{m_i^2(\phi)}{m_i^2(v)} \right) - \frac{3}{2} \right) + 2m_i^2(\phi)m_i^2(v) \right], \quad (32)$$

where g_i is the number of d.o.f. of each particle species, $m_i(\phi)$ is the ϕ -dependent mass, and the upper and lower signs correspond to bosons and fermions, respectively. The one loop finite-temperature corrections to the free energy density, including the resummed

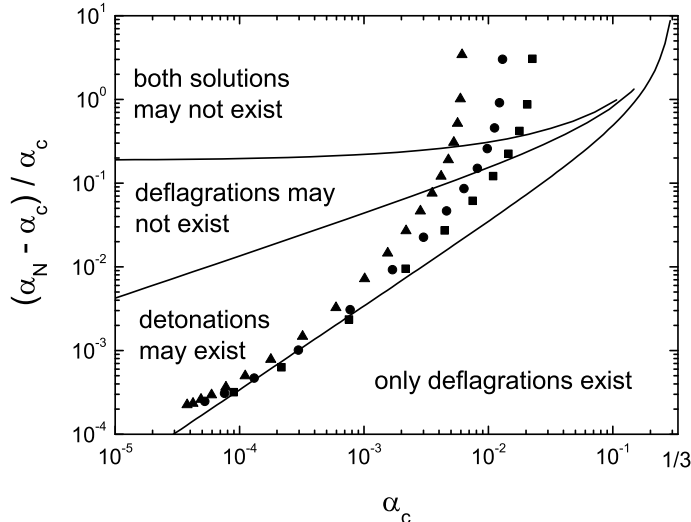


Figure 9: The regions of the plane (α_c, α_N) where detonations and deflagrations may or may not exist. The points correspond to the model of section 4, for different values of the d.o.f. g and coupling h . Triangles correspond to $g = 2$, circles to $g = 6$, and squares to $g = 12$.

daisy diagrams are

$$\begin{aligned} \mathcal{F}_1(\phi, T) &= \sum_i \frac{\pm g_i T^4}{2\pi^2} \int_0^\infty dx x^2 \log \left[1 \mp \exp \left(-\sqrt{x^2 + m_i^2(\phi)}/T \right) \right] \\ &+ \sum_{\text{bosons}} \frac{g_i T}{12\pi} [m_i^3(\phi) - \mathcal{M}_i^3(\phi)], \end{aligned} \quad (33)$$

where the upper sign stands for bosons, the lower sign stands for fermions, and $\mathcal{M}_i^2(\phi) = m_i^2(\phi) + \Pi_i(T)$, where $\Pi_i(T)$ are the thermal masses. The last term receives contributions from all the bosonic species except the transverse polarizations of the gauge bosons. Hence, the one-loop finite-temperature effective potential is of the form

$$\mathcal{F}(\phi, T) = V_0(\phi) + V_1(\phi) + \mathcal{F}_1(\phi, T) + \rho_\Lambda, \quad (34)$$

where we have added a constant $\rho_\Lambda = -V_0(v) - V_1(v)$, so that at $T = 0$ we will not have a vacuum energy density of order v^4 in the true vacuum. Thus, we have $\rho_-(T = 0) = 0$. If all the masses m_i vanish in the symmetric phase, the constant ρ_Λ gives the false vacuum energy density $\rho_+(T = 0)$.

For the SM, the relevant contributions come from the Z and W bosons and the top quark. The top quark contributes with $g_t = 12$ fermionic d.o.f., with a mass $m_t(\phi) = h_t \phi / \sqrt{2}$, where h_t is the Yukawa coupling ($h_t / \sqrt{2} \approx 0.7$). For the weak gauge bosons, it can be seen numerically [30] that a good approximation for the one-loop correction is to consider a single mass of the form $m_b(\phi) = h_b \phi$, with $h_b \approx 0.35$, and $g_b = 6$ bosonic d.o.f. The rest of the SM d.o.f. have $h_i \ll 1$ and only contribute a ϕ -independent term $-\pi^2 g_{\text{light}} T^4 / 90$, with $g_{\text{light}} \approx 90$. Each extra complex field S gives contributions to the free energy of the form (32,33), with $g_S = 2$ d.o.f. and a mass of the form $m^2(\phi) = h^2 \phi^2 + \mu^2$.

The thermal mass is given by $\Pi = h^2 T^2/3 + \lambda_S/4$. For simplicity, in this work we shall set $\mu = \lambda_S = 0$. For illustrative purposes, we shall also fix the Higgs mass to the value $m_H = 125 \text{ GeV}$. It is well known that increasing the Higgs mass weakens the phase transition. Therefore, higher masses give lower values of v_w . The same happens for nonzero values of the boson mass parameter μ since, as μ is increased, the extra bosons decouple from the thermal system and the phase transition becomes weaker. In a forthcoming paper [35] we will consider several particular (and physically motivated) extensions of the SM.

4.2 Critical temperature and latent heat

We can find the symmetry-breaking minimum $\phi_m(T)$ for the free energy (34) by demanding $\partial\mathcal{F}(\phi, T)/\partial\phi = 0$. Then, as we have seen in section 1, we define the functions $\mathcal{F}_+(T) = \mathcal{F}(0, T)$ and $\mathcal{F}_-(T) = \mathcal{F}(\phi_m(T), T)$. From these, we calculate the critical temperature through the condition $\mathcal{F}_+(T_c) = \mathcal{F}_-(T_c)$, and the latent heat by

$$L = T_c (\mathcal{F}'_-(T_c) - \mathcal{F}'_+(T_c)). \quad (35)$$

Analytic expressions can be obtained by considering the high-temperature expansion of the thermal integrals appearing in (33). However, this approximation breaks down for $m_i(\phi)/T \gg 1$. In our model this corresponds to strong phase transitions, with $h\phi/T \gg 1$. Therefore, we shall calculate numerically T_c and L .

The energy density of the high-temperature phase can be derived from the free energy density (34) by the relation $\rho_+ = \mathcal{F}_+(T) - T\mathcal{F}'_+(T)$. The thermal energy density is given by $\tilde{\rho}_+ = \rho_+ - \rho_\Lambda$. In general, we have $\tilde{\rho}_+ \approx \pi^2 g_* T^4/30$, where g_* is the number of relativistic d.o.f. Thus we can readily calculate the parameter $\alpha_c = L/\tilde{\rho}_+(T_c)$. In order to calculate the parameter $\alpha_N = L/\tilde{\rho}_+(T_N)$, we need to compute the temperature T_N at which bubbles nucleate. The latent heat parameter L in α_N must be the same as in α_c , since for the bag equation of state the released energy does not depend on temperature. Therefore, in order to apply the results of the previous sections, we must use Eq. (35) for the computation of α_N , which gives the correct relation $\alpha_N/\alpha_c = (T_c/T_N)^4$. If we used instead the energy that is released at $T = T_N$, which is larger, we would be overestimating the velocity, since for the bag EOS this would be equivalent to considering a stronger supercooling.

4.3 The Nucleation temperature

In a first-order phase transition, the nucleation of bubbles is governed by the three-dimensional instanton action

$$S_3 = 4\pi \int_0^\infty r^2 dr \left[\frac{1}{2} \left(\frac{d\phi}{dr} \right)^2 + V(\phi(r), T) \right], \quad (36)$$

where $V(\phi, T) \equiv \mathcal{F}(\phi, T) - \mathcal{F}(0, T)$. The bounce solution of this action, which is obtained by extremizing S_3 , gives the radial configuration of the nucleated bubble, assumed to be spherically symmetric. The action of the bounce coincides with the free energy of a critical

bubble (i.e., a bubble in unstable equilibrium between expansion and contraction). The bounce solution obeys the equation

$$\frac{d^2\phi}{dr^2} + \frac{2}{r} \frac{d\phi}{dr} = V'(\phi) \quad (37)$$

with boundary conditions

$$\frac{d\phi}{dr}(0) = 0, \quad \lim_{r \rightarrow \infty} \phi(r) = 0. \quad (38)$$

The thermal tunneling probability for bubble nucleation per unit volume and time is [9]

$$\Gamma(T) \simeq A(T) e^{-S_3(T)/T}, \quad (39)$$

with $A(T) = [S_3(T)/2\pi T]^{3/2}$.

The nucleation temperature T_N is defined as that at which the probability of finding a bubble in a causal volume is 1,

$$\int_{t_c}^{t_N} dt \Gamma(T) V = 1, \quad (40)$$

where t_c is the time at which the Universe reaches the critical temperature T_c and t_N is the time at which the first bubbles are nucleated in a causal volume V . In the radiation-dominated era we have $V \sim (2t)^3$, and the time-temperature relation is given by³

$$dT/dt = -HT, \quad (41)$$

where H is the expansion rate, $H = \sqrt{8\pi G\rho_+(T)}/3$. Here, G is Newton's constant. If $\rho_+ \approx \tilde{\rho}_+ \approx \pi^2 g_* T^4/30$, then the time-temperature relation is given by the usual expression $t = \xi M_P/T^2$, where M_P is the Planck mass and $\xi = \sqrt{45/(16\pi^3 g_*)}$.

The nucleation rate $\Gamma(T)$ can be calculated by solving numerically Eq. (37) for the bubble profile, then integrating Eq. (36) for the bounce action and, finally, using the result in Eq. (39). Analytical approximations to Eqs. (36-39) have large errors due to the exponential dependence of Γ and the sensitivity of S_3 to temperature. We solved Eq. (37) iteratively by the overshoot-undershoot method⁴.

4.4 The friction coefficient

The effect of microphysics on the propagation of the bubble wall can be calculated by considering the equation for the Higgs field in the hot plasma. From energy conservation considerations, one can derive the equation

$$\partial_\mu \partial^\mu \phi + \frac{\partial \mathcal{F}(\phi, T)}{\partial \phi} + \sum_i g_i \frac{\partial m_i^2}{\partial \phi} \int \frac{d^3 p}{(2\pi)^3} \frac{1}{2E_i} \delta f_i = 0, \quad (42)$$

³This relation may change due to reheating during the development of the phase transition, for $t > t_N$ [4, 30, 36].

⁴See Ref. [30] for details.

where the sum is over all particle species that couple with ϕ , m_i are the ϕ -dependent masses, and δf_i are the deviations from the equilibrium distribution functions, induced by the motion of the wall. The deviations δf_i have been calculated either using kinetic theory [11, 12, 13, 14], or considering infrared excitations of bosonic fields [15], which undergo overdamped evolution [16].

Calculations of the friction are usually carried out *ignoring hydrodynamics* (i.e., disregarding temperature and velocity profiles of the fluid). Assuming stationary motion in the z direction, the first term in Eq. (42) becomes $(v_w^2 - 1) \phi''(z)$, and the deviations δf_i near the wall depend on $\phi(z)$ and $\phi'(z)$. To the lowest order, δf_i is proportional to the wall velocity v_w . As a consequence, if we multiply by $\phi'(z)$ and integrate over $-\infty < z < +\infty$, we obtain

$$\mathcal{F}(0, T) - \mathcal{F}(\phi_m, T) = \eta v_w, \quad (43)$$

where η is a friction coefficient which depends on the particle content of the plasma. For particles with a thermal distribution we have [17]

$$\eta_{\text{th}} \sim \sum \frac{3g_i h_i^4}{(\Gamma_i/10^{-1}T)} \left(\frac{\log \chi_i}{2\pi^2} \right)^2 \frac{\phi_m^2 \sigma}{T}, \quad (44)$$

where g_i is the number of degrees of freedom of species i , h_i is the coupling to ϕ , Γ_i are interaction rates which are typically $\lesssim 10^{-1}T$, $\chi_i = 2$ for fermions and $\chi_i = h_i^{-1}$ for bosons, while infrared bosons give a contribution [16]

$$\eta_{\text{ir}} \sim \sum \frac{g_b}{32\pi} \left(\frac{m_D}{T} \right)^2 \log(m_b(\phi_m) L_w) \frac{T^3}{L_w}, \quad (45)$$

where g_b is the number of bosonic degrees of freedom, L_w is the width of the bubble wall, and m_D is the Debye mass, given by $m_D^2 \sim h_b^2 T^2$, where h_b is the coupling to ϕ .

For bosonic d.o.f., expressions (44) and (45) dominate in different ranges of the couplings h_b , and we shall assume $\eta = \eta_{\text{th}} + \eta_{\text{ir}}$. Both expressions involve several approximations and have $\mathcal{O}(1)$ errors, but should be parametrically correct.

4.4.1 Parametrization of the friction

To relate the friction coefficient η obtained from microscopical calculations to the one we used as a free parameter in the previous sections, compare Eqs. (43-45) with Eqs. (8,9) [36]. We see that the thermal friction coefficient (44) can be written in the form $\eta = \tilde{\eta} T_c \sigma$, with

$$\tilde{\eta}_{\text{th}} = \sum \frac{3g_i h_i^4}{(\Gamma_i/10^{-1}T)} \left(\frac{\log \chi_i}{2\pi^2} \right)^2 \left(\frac{\phi_m}{T} \right)^2. \quad (46)$$

The surface tension is roughly given by $\sigma \approx \phi_m^2/L_w$. Furthermore, in general we have $\phi_m \sim T$. Therefore, the last factor in Eq. (45) becomes $T^3/L_w \sim T\sigma$. Thus, the infrared boson contribution can also be written in the form (9), with

$$\tilde{\eta}_{\text{ir}} = \sum_{\text{gauge}} \frac{g_b}{32\pi} \left(\frac{m_D}{T} \right)^2 \log(m_b(\phi_m) L_w). \quad (47)$$

Thus, for a given model, we can estimate the value of $\tilde{\eta}$ in Eq. (9) using Eqs. (46,47).

4.5 Numerical results

We have numerically calculated the values of α_c , α_N and η/L for this model, as functions of the coupling h and the number of d.o.f. g of the scalar singlets. From these, we have calculated the wall velocity v_w at $T = T_N$, using the results of section 3.

In Fig. 10 we have plotted the value of the deflagration wall velocity as a function of h for $g = 2$. Since the phase transition strengthens with h , one would expect the wall velocity to be a monotonically increasing function of h (perhaps eventually bounded by c_s). Indeed, roughly we have $v_w(T_N) \sim \Delta\mathcal{F}(T_N)/\eta$, so v_w is dominated by the amount of supercooling and by the friction. The friction coefficients η_{th} and η_{ir} oscillate for $h \sim 1$ due to the log terms in Eqs. (44) and (45). This causes a minimum and a maximum in the wall velocity. For large h , the friction coefficient η_{th} dominates since it goes like h^4 , and the velocity finally decreases. To illustrate this effect, we have plotted in Fig. 10 the value of the friction coefficient $\tilde{\eta} = \tilde{\eta}_{\text{th}} + \tilde{\eta}_{\text{ir}}$.

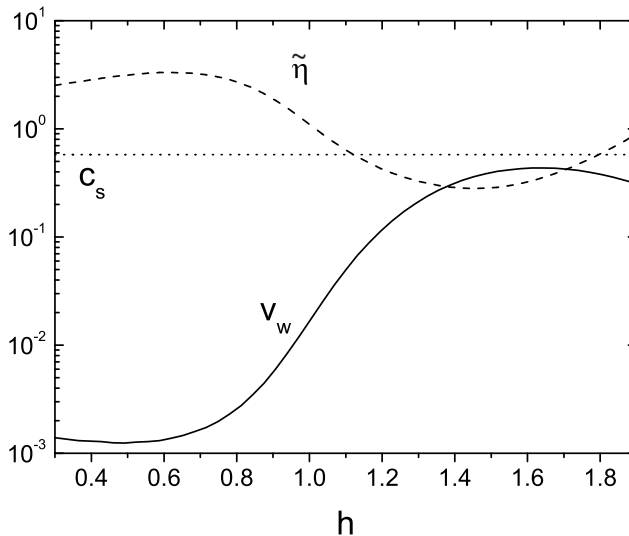


Figure 10: The wall velocity and friction coefficient as functions of the coupling h for $g = 2$ d.o.f.

Figure 11 shows the deflagration wall velocity as a function of the coupling h for the cases $g = 2$, $g = 6$, and $g = 12$. The crosses in the $g = 12$ curve indicate the points where $\phi(T_N)/T_N \approx 1$ and $\phi(T_N)/T_N \approx 2$. (These points were taken as a reference for the variation of the parameters in the previous section.) For each g , the calculation was done up to a value $h = h_{\text{max}}$ for which the time required to get out of the supercooling stage becomes too long for the numerical computation. This happens because the phase transition becomes so strong that the barrier between minima persists at low temperatures, and the nucleation temperature quickly falls to zero. Indeed, near this endpoint, the free energy has a barrier between minima already at $T = 0$. For h beyond $h = h_{\text{max}}$, the temperature T_c also goes to 0. The dependence on the coupling will not be so strong if fermions are added to the model (see e.g. Fig. 6 of Ref. [30]).

Notice that the deflagration wall velocity can reach the speed of sound c_s only for large enough g and the largest values of h in each curve, corresponding to really strong

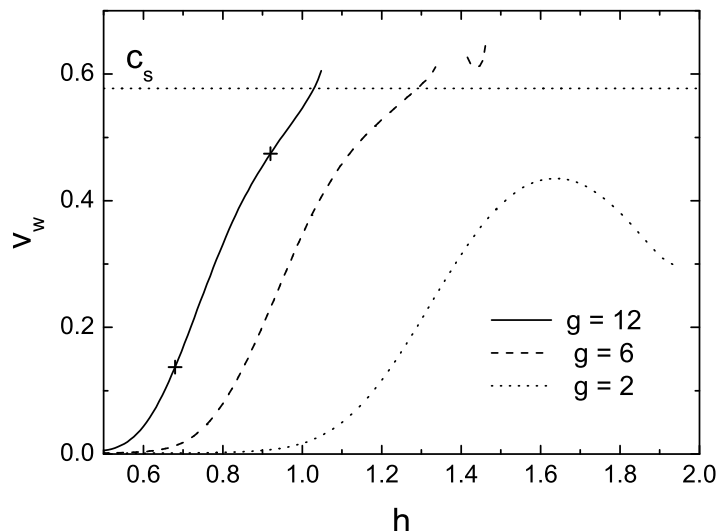


Figure 11: The wall velocity as a function of h .

phase transitions. Immediately after crossing the line of $v_w = c_s$, the deflagration solution may disappear (cases $g = 6$ and $g = 12$ in the figure), and it may reappear (case $g = 6$), indicating a borderline case in parameter space. For the case $m_H = 125\text{GeV}$, we have considered values of g_b in the range $0 - 20$, varying h up to h_{max} for each g , and we have not found detonation solutions. This occurs because, although the supercooling increases with h , the friction increases as well. For lower Higgs masses, namely, $m_H = 100\text{GeV}$, detonation solutions appear only for $h \approx h_{\text{max}}$.

Figure 9 shows the values of α_c and α_N corresponding to the curves of Fig. 11. Lower values of h give weaker phase transitions and, hence, lower values of α_c and α_N . As h becomes large, the supercooling diverges before α_c reaches the limiting value $1/3$. Most points, though, are close to the region where detonations do not exist. For these cases, detonations would exist only for very low values of the friction. On the other hand, for large h the points move away from the lowest curve in Fig. 9. For these points, the supercooling is quite larger than the minimum that is needed for the existence of detonations. Therefore, one expects that this kind of solution would appear if the friction were a little smaller. As we already mentioned, the error in the calculation of the friction is a $\mathcal{O}(1)$ factor. Thus, we also consider a friction which is a factor of 2 larger and a factor of 2 smaller than the value given by Eqs. (44,45). The result is shown in Fig. 12. In the case $\eta/2$ we obtain detonations for large values of h , if g is large enough.

5 Analytic approximations for the wall velocity

Analytic approximations for the wall velocity are very useful for cosmological applications. Two approximations are commonly used. In the case of deflagrations, if one ignores hydrodynamics, the wall velocity can be obtained by equating the pressure difference Δp between phases (which pushes the wall towards the high-temperature phase) to a friction force per unit area, which is typically proportional to the velocity, $f = \eta v_w$.

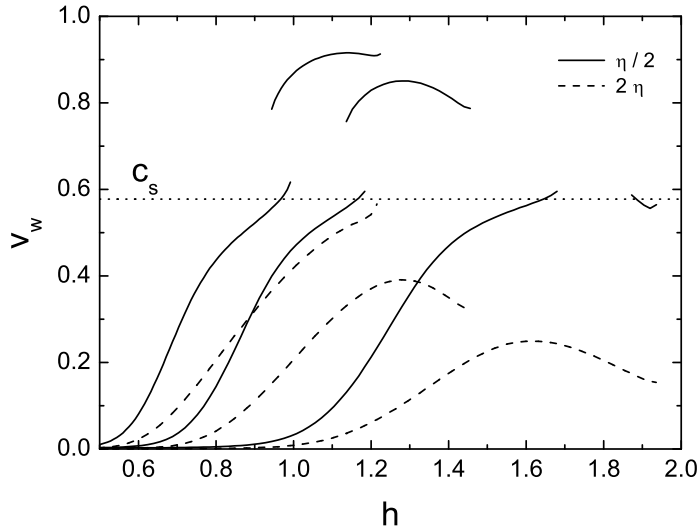


Figure 12: Same as for Fig. 11, but considering a larger and a smaller friction parameter (from left to right, the curves correspond to $g = 12, 6,$ and 2).

Thus, one obtains the well known result $v_w = \Delta p(T)/\eta$, which has been widely used in electroweak baryogenesis [11, 12, 13, 14, 15, 16, 17]. This velocity depends on the amount of supercooling, since $\Delta p = 0$ at the critical temperature, and gives a good approximation for nonrelativistic velocities. However, ignoring hydrodynamics overestimates the value of v_w , since the released latent heat accumulates in front of the wall, causing a slow-down of the wall velocity. Nevertheless, if the friction is large enough, this effect is negligible.

In the case of detonations, the Chapman-Jouguet condition, $v_- = c_s$, leads to the simple formula

$$v_J(\alpha) = \frac{\sqrt{1/3} + \sqrt{\alpha^2 + 2\alpha/3}}{1 + \alpha}, \quad (48)$$

which is obtained by setting $v_- = 1/\sqrt{3}$ in Eq. (3). This formula has been widely used for the calculation of gravitational radiation [5, 6, 34]. However, as we have already mentioned, it is rather strange that Eq. (48) does not depend on microphysics. Furthermore, it depends only on the ratio $L/\tilde{\rho}_+(T_N)$. This means that increasing the latent heat will cause the same effect as decreasing T_N , which is to increase the wall velocity. It is true that the pressure difference goes like the product $L(T_c - T_N)$, but, on the other hand, increasing L will enlarge the effect of hydrodynamics, which is to slow down the wall. As we shall see, the velocity decreases if L is increased with the amount of supercooling held fixed⁵. As can be seen in Fig. 4, according to our results, the Jouguet velocity is a bad approximation to the detonation velocity (it approximates well the non-physical solution).

In this section we shall derive analytical approximations both for the detonation and the deflagration, by taking the ultrarelativistic and nonrelativistic limits, respectively, of the equations obtained in section 2. Before going on, though, one further comment is

⁵In a particular model, increasing L will give in general more supercooling. However, such a relation cannot be derived from hydrodynamics alone, but from calculating the nucleation rate.

worth. As we have seen, the parameter ε in $\alpha = \varepsilon/\tilde{\rho}_+$ is not given by the latent heat L , but by $\varepsilon = L/4$. This fact was already mentioned in earlier works on gravitational waves [5]. However, the vacuum energy density ε is sometimes confused with the latent heat L . When analytical results are used for a particular model, this amounts to considering a value of α four times larger than the actual value, which leads to an overestimation of the detonation velocity.

5.1 The ultrarelativistic limit

For $v_w \approx 1$, we can write $v_w = 1 - \delta$, with $\delta \ll 1$. In this limit we must consider detonations, for which $v_w = |v_+|$ and $\alpha_+ = \alpha_N \equiv \alpha$. Therefore, we have $|v_+| = 1 - \delta$ and, from Eq. (3), $|v_-| = 1 - \delta(1 + 3\alpha) + \mathcal{O}(\delta^2)$. To lowest order in δ , we have $|v_+|\gamma_+ = 1/\sqrt{2\delta}$ and $|v_-|\gamma_- = 1/\sqrt{2\delta(1 + 3\alpha)}$. Thus, the last term in Eq (20) is $\sim 1/\sqrt{\delta}$. For the first term we have, from Eq. (21), $(p_+ - p_-)/\rho_+ = -2\alpha + \mathcal{O}(\delta)$. The second term is obtained from Eqs. (22) and (23). From Eq. (23) we have $\rho_-/\rho_+ = 1 + 3\alpha + \mathcal{O}(\delta)$, from which we obtain $T_-/T_+ = (a_-/a_+)^{-1/4}(1 + 3\alpha)^{1/4} + \mathcal{O}(\delta)$, and $s_-/s_+ = (a_-/a_+)^{1/4}(1 + 3\alpha)^{3/4} + \mathcal{O}(\delta)$. Inserting these results in Eq. (20) we obtain, to lowest order⁶,

$$\begin{aligned} v_w &= 1 - \delta, \\ \sqrt{2\delta} &= \frac{(3/4)(\sqrt{1 + 3\alpha} + 1)\bar{\eta}}{r^{1/4}(1 + 3\alpha)^{5/4} - r^{-1/4}(1 + 3\alpha)^{3/4}}, \end{aligned} \quad (49)$$

with $\alpha = \varepsilon/(a_+T_N^4)$, $\bar{\eta} = \eta/(a_+T_N^4)$, and $r \equiv a_-/a_+ = 1 - 3\alpha_c$, with $\alpha_c = \varepsilon/(a_+T_c^4)$. We remind also that the correct relation between ε and L is $\varepsilon = L/4$.

Since the detonation velocity is usually large ($v_w \geq 0.8$), the simple formula (49) turns out to be an excellent approximation in general. We have plotted this approximation in Fig. 13 together with the numerical result, for the same detonation curves of the right panel of Fig. 6. For comparison, the Jouguet velocity lies below 0.7 (and is constant for α fixed). Since the parameter δ is bounded by $1 - c_s \approx 0.4$, we expect Eq. (49) to give a good approximation in all the possible range of the detonation velocity.

It is interesting to consider some limiting cases of Eq. (49). For $\eta \rightarrow 0$ with all the other quantities held fixed, the wall velocity approaches the speed of light. However, for any finite value of η , the denominator diverges at $\alpha_N/\alpha_c = a_+/a_- = 1/(1 - 3\alpha_c)$. Hence, α_N has a lower bound larger than α_c (except in the limit $\alpha_c \rightarrow 0$). This divergence reflects the fact that a certain amount of supercooling is always needed for detonations to exist. As a consequence, we cannot take the limit of small supercooling, $\alpha_N/\alpha_c \approx 1$.

If we increase L with fixed α_N and η , it can be easily seen from Eq. (49) that v_w decreases. This is because increasing L strengthens the effect of hydrodynamics, which is to slow-down the wall. Taking the limit of large L is not very useful. In the first place, L

⁶Keeping the next order in the equation is straightforward, and leads to

$$\sqrt{\delta} = \frac{\sqrt{\frac{32}{9}D^2 - \bar{\eta}^2(4q + 3q^{1/2} + 1 - 2/q)(q^{1/2} + 1) - \frac{4\sqrt{2}}{3}D}}{(\bar{\eta}/2)(4q + 3q^{1/2} + 1 - 2/q)},$$

where D is the denominator in Eq. (49) and $q = 1 + 3\alpha$.

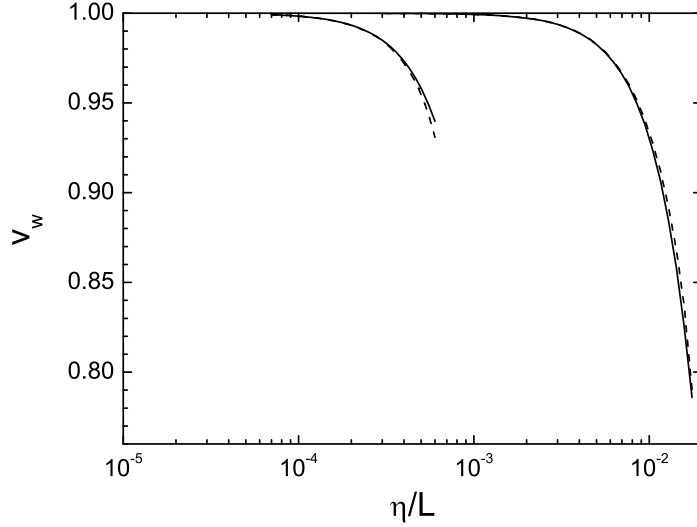


Figure 13: The analytical approximation (49) (dashed line) together with the numerical result (solid line), for the detonation solutions of Fig. 6, right.

is bounded by $(4/3)\tilde{\rho}_+(T_c)$ (we remark that this is a general thermodynamical constraint [30]). Hence, this limit corresponds to taking $\alpha_c \rightarrow 1/3$ (or $a_- \rightarrow 0$). However, this is the limit of an extremely strong phase transition which, in a realistic model will have also $T_N \rightarrow 0$ (or $\alpha_N \rightarrow \infty$). Conversely, the limit of large supercooling, $\alpha_N/\alpha_c \rightarrow \infty$, should be taken together with $\alpha_c \rightarrow 1/3$. It is not straightforward how to take this limit in Eq. (49), since the bag model does not provide a way to calculate the nucleation temperature T_N .

On the other hand, we can consider the limit $L \rightarrow 0$. In this case both α_c and $\alpha_N \rightarrow 0$, (unless $T_N \ll T_c$, which will not be the case in a realistic model if L is small). Hence, Eq. (49) yields $\sqrt{2\delta} \approx (\eta/\tilde{\rho}_+)/(\alpha_N - \alpha_c) = (4\eta/L)/(1 - T_N^4/T_c^4)$. From Eqs. (16-18), we see that $L(1 - T_N^4/T_c^4)/4 = p_-(T_N) - p_+(T_N)$. Since in the ultrarelativistic limit we have $1/\sqrt{2\delta} = v_w\gamma_w$, we obtain $v_w\gamma_w = \Delta p(T_N)/\eta$. Thus, as expected, in the limit $L \rightarrow 0$ we can neglect the effects of hydrodynamics. The wall velocity becomes, according to Eq. (49), $v_w = 1 - \frac{1}{2}(\eta/\Delta p(T_N))^2$.

5.2 The nonrelativistic limit

In the nonrelativistic limit $v_w \ll 1$, we must consider deflagrations. Thus, we have $|v_-| = v_w$, and Eq. (3) becomes $v_+ = (1 - 3\alpha_+)v_- + \mathcal{O}(v_w^2)$. Therefore, according to Eq. (21), we have $(p_+ - p_-)/\tilde{\rho}_+ = \mathcal{O}(v_w^2)$ and, by Eq. (23), $\rho_-/\tilde{\rho}_+ = 1 - 3\alpha_+ + \mathcal{O}(v_w^2)$. Thus, $T_-/T_+ = (a_-/a_+)^{-1/4}(1 - 3\alpha_+)^{1/4} + \mathcal{O}(v_w^2)$ and $s_-/s_+ = (a_-/a_+)^{1/4}(1 - 3\alpha_+)^{3/4} + \mathcal{O}(v_w^2)$. To lowest order in v_w , Eq. (20) becomes

$$3\alpha_+(2 - 3\alpha_+)\frac{\eta}{L}v_w = \left(\frac{a_-}{a_+}\right)^{1/4}(1 - 3\alpha_+)^{3/4} - \left(\frac{a_-}{a_+}\right)^{-1/4}(1 - 3\alpha_+)^{1/4} + 3\alpha_+. \quad (50)$$

In the case of deflagrations, we must also find α_+ as a function of α_N . In this approximation, $v_+ - v_-$ is given by $3\alpha_+v_w$. Hence, according to Eq. (30), $\alpha_N - \alpha_+$ is of order

v_w , and so the left hand side becomes $\sqrt{3}(\alpha_N - \alpha_+)/ (4\alpha_N)$. Thus, to lowest order in v_w , Eq. (30) gives $\alpha_+ = \alpha_N - 4\sqrt{3}\alpha_N^2 v_w$. Inserting this in Eq. (50) and discarding higher order terms, we obtain

$$v_w = \frac{(1 - 3\alpha)^{\frac{3}{4}} \left(3\alpha - r^{-\frac{1}{4}} (1 - 3\alpha)^{\frac{1}{4}} + r^{\frac{1}{4}} (1 - 3\alpha)^{\frac{3}{4}} \right)}{\frac{3}{4}\bar{\eta} (2 - 3\alpha) (1 - 3\alpha)^{\frac{3}{4}} + 3\sqrt{3}\alpha^2 \left[r^{-\frac{1}{4}} + 4(1 - 3\alpha)^{\frac{3}{4}} - 3r^{\frac{1}{4}} (1 - 3\alpha)^{\frac{1}{2}} \right]}, \quad (51)$$

where $\alpha \equiv \alpha_N = (L/4) / (a_+ T_N^4)$, $\bar{\eta} = \eta / (a_+ T_N^4)$, and $r \equiv a_- / a_+ = 1 - 3\alpha_c$, with $\alpha_c = (L/4) / (a_+ T_c^4)$.

The appearance of factors $(1 - 3\alpha_N)^{1/4}$ indicates the fact that the deflagration solution cannot exist for α_N arbitrarily large. For $\eta \rightarrow 0$, only the first term in the denominator vanishes; the velocity will not necessarily be large, nor the approximation break-down. This reflects the fact that hydrodynamics slows down the motion of the bubble wall. For $L \rightarrow 0$, i.e., $\alpha_c, \alpha_N \rightarrow 0$, we obtain, similarly to the detonation case, $v_w = \Delta p(T_N) / \eta$, which corresponds to neglecting hydrodynamics. It is interesting to consider also, without neglecting hydrodynamics, the case in which Δp is small, i.e, the limit of small supercooling.

5.2.1 Small supercooling

In the nonrelativistic limit, the pressure difference $p_+ - p_-$ is $\mathcal{O}(v_w^2)$. This can be seen already from the nonrelativistic version of Eqs. (1),

$$w_+ v_+ = w_- v_-, \quad w_+ v_+^2 + p_+ = w_- v_-^2 + p_-. \quad (52)$$

On the other hand, according to Eq. (13), the temperature difference $T_+ - T_-$ is $\mathcal{O}(\eta v_w)$. We shall now consider the case in which η is not too small, so that the temperature difference must be $T_+ - T_- = \mathcal{O}(v_w)$. This means that, to order v_w , the pressure difference due to supercooling, $p_- - p_+ \sim T_c - T$, is canceled by the pressure difference due to the temperature gradient, $p_- - p_+ \sim T_- - T_+$. Hence, the differences $T_c - T_{\pm}$ must be also $\mathcal{O}(v_w)$. Thus, in this case we can expand the thermodynamic quantities to first order in $T - T_c$. In particular, for the pressure functions we have $p_{\pm}(T) = p_{\pm}(T_c) + s_{\pm}(T_c)(T - T_c)$, which can be used instead of the equations of state (16). Thus, we can write

$$p_+(T_+) - p_-(T_-) = (s_+ - s_-)(T_+ - T_c) + s_-(T_+ - T_-), \quad (53)$$

where s_+ and s_- are evaluated at $T = T_c$. Therefore we have

$$T_+ - T_- = \frac{\Delta s}{s_-} (T_c - T_+) + \mathcal{O}(v_w^2). \quad (54)$$

To first order in v_w , we neglect the first term in Eq. (13) and, inserting Eq. (54) in the second term, we obtain

$$L \frac{T_c - T_+}{T_c} = \frac{s_-}{s_+} \eta v_w, \quad (55)$$

where we have used $L = T_c (s_+ - s_-)$ and $v_+ = (w_-/w_+)v_-$, with $|v_-| = v_w$.

If we had $T_+ = T_N$, this would only give a correction of a factor s_+/s_- to the usual equation $v_w = \Delta p(T)/\eta$. However, an important contribution comes from the fluid that is accumulated in front of the moving wall. For T_+ and $T_N \approx T_c$, the relation (30) between the nucleation temperature T_N and that of the reheated fluid T_+ is given by

$$\frac{T_+ - T_N}{T_c} = \frac{v_w L}{\sqrt{3}w_+}, \quad (56)$$

where the enthalpy w_+ is evaluated at $T = T_c$. We finally obtain

$$v_w = \frac{(w_+/w_-)(T_c - T_N)/T_c}{\eta/L + L/(\sqrt{3}w_-)}, \quad (57)$$

which agrees with the result of Ref. [10]. Comparing with Eq. (8) and taking into account that $\Delta\mathcal{F}(T) \approx L(T_c - T)/T_c$, we may write

$$v_w = \frac{L(T_c - T_N)/T_c}{\eta_{\text{eff}}}, \quad (58)$$

where the effective friction coefficient

$$\eta_{\text{eff}} = \frac{w_-}{w_+} \left(\eta + \frac{L^2}{\sqrt{3}w_-} \right) \quad (59)$$

includes the effects of hydrodynamics. If friction dominates, i.e., if $\eta/L \gg L/(\sqrt{3}w_-)$, we obtain $v_w = (w_-/w_+)L(T_c - T_N)/\eta$. For $L \ll \rho_+$, we have $w_- \approx w_+$, and we recover Eq. (8). In the opposite limit, i.e., for $\eta/L \ll L/(\sqrt{3}w_-)$, we still obtain a finite velocity $v_w = (4\rho_+/L)(T_c - T_N)$. Again, this means that the latent heat that is accumulated in front of the bubble wall slows down the motion of the wall.

In Fig. 14 we plot the two approximations for deflagrations, together with the numerical result and the usual approximation which neglects hydrodynamics. As expected, the numerical calculation gives smaller values of v_w than the analytical approximations, since the exact velocity has an upper bound, namely, the speed of light. We see that in general the nonrelativistic approximation is quite good up to $v_w \approx 0.4$, and breaks down for $v_w \gtrsim c_s$. Notice that a useful, rough approximation consists of assuming that v_w is given by, say, Eq. (57) up to $v_w = c_s$, and by $v_w = c_s$ when Eq. (57) becomes supersonic.

6 Conclusions

We have studied the steady state velocity of bubble walls in first-order cosmological phase transitions. We have numerically investigated the whole velocity range $0 < v_w < 1$, and we have found analytic approximations for the limits $v_w \ll 1$ and $v_w \approx 1$.

Thus, we have considered both detonations and deflagrations. We have derived a relatively simple set of equations for the wall velocity and the fluid variables on both sides of the wall. To obtain these equations we have used three ingredients, namely, the

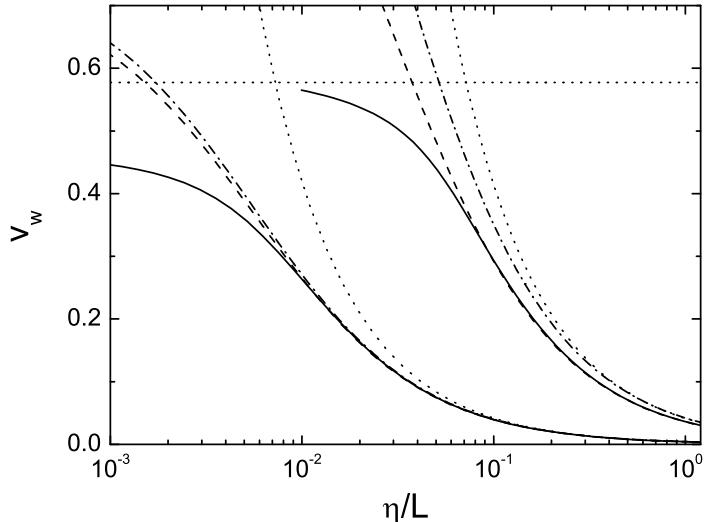


Figure 14: The various analytical approximations for deflagrations. Solid line: the numerical result. Dashed line: the nonrelativistic approximation of Eq. (51). Dashed-dotted line: the approximation of Eq. (57) for small supercooling. Dotted line: the usual approximation $v_w = \Delta p/\eta$.

continuity conditions for the fluid variables at the phase transition front (and at the shock front in the case of deflagrations), the introduction of a damping term in the equation of motion for the order parameter (Higgs field), and the bag equation of state. The parametrization of the friction provides a model-independent equation which involves a friction parameter η . We obtained this equation by generalizing a procedure used in Ref. [10] for the case of nonrelativistic velocities and small supercooling. We have also shown how to calculate the parameter η in a specific model.

We have solved numerically these equations for the wall velocity as a function of the parameters α_c , α_N and η/L which depend essentially on the latent heat L , the nucleation temperature T_N , and the friction coefficient η . We have studied the regions in parameter space where detonations and deflagrations are possible, and we have also considered a specific model (the Standard Model with extra singlet scalar fields) to investigate how a physical case moves about through these regions.

We have found that supersonic velocities (either detonations or deflagrations) are in general obtained only for very strong phase transitions, with $\phi(T_N)/T_N > 2$, occurring in the model for relatively large values of the number of scalar singlets g and of their coupling h to the Higgs. Besides, the existence of detonations requires relatively low values of the friction, and it may happen that for such strong phase transitions neither detonations nor deflagrations exist. In such a case, the steady state cannot be reached, and the wall will accelerate until bubbles collide. The case in which the wall velocity gets close to the speed of light before bubble collision may have important implications for gravitational wave generation. Interestingly, this ultrarelativistic situation has been considered very recently [37] for the SM extension with singlet scalar fields, finding that such “runaway” solutions exist for very strong phase transitions.

In a more general extension of the SM, the singlets may have a ϕ -independent mass

term, which will weaken the phase transition. In that case, detonations may not appear at all. The inclusion of fermions in the model will also weaken the phase transition, but the friction coefficient will not have the infrared contribution and will be smaller. In a forthcoming paper [35] we shall investigate several extensions of the SM, including the MSSM and an extension with strongly coupled fermions [38].

Finally, we have discussed the validity of commonly used analytical approximations for the wall velocity, and we have obtained nonrelativistic and ultrarelativistic approximations. In particular, we have shown that the Jouguet velocity gives a really bad approximation to detonations; the actual detonation velocity is quite larger. We have found an alternative approximation (49) which, besides being more realistic, is quite simple and gives an excellent fit to the numerical result.

Acknowledgements

This work was supported in part by Universidad Nacional de Mar del Plata, Argentina, grants EXA 365/07 and 425/08. The work by A.D.S. was supported by CONICET through project PIP 5072. The work by A.M. was supported by FONCyT grant PICT 33635.

References

- [1] For reviews, see A. G. Cohen, D. B. Kaplan and A. E. Nelson, *Ann. Rev. Nucl. Part. Sci.* **43**, 27 (1993) [arXiv:hep-ph/9302210]; A. Riotto and M. Trodden, *Ann. Rev. Nucl. Part. Sci.* **49**, 35 (1999) [arXiv:hep-ph/9901362].
- [2] D. Grasso and H. R. Rubinstein, *Phys. Rept.* **348**, 163 (2001) [arXiv:astro-ph/0009061].
- [3] A. Vilenkin and E.P.S. Shellard, *Cosmic Strings and Other Topological Defects* (Cambridge University Press, Cambridge, England, 1994).
- [4] A. F. Heckler, *Phys. Rev. D* **51** (1995) 405 [arXiv:astro-ph/9407064]; E. Witten, *Phys. Rev. D* **30**, 272 (1984); A. Mégevand and F. Astorga, *Phys. Rev. D* **71**, 023502 (2005).
- [5] M. Kamionkowski, A. Kosowsky and M. S. Turner, *Phys. Rev. D* **49**, 2837 (1994).
- [6] A. Kosowsky, A. Mack and T. Kahniashvili, *Phys. Rev. D* **66**, 024030 (2002); A. D. Dolgov, D. Grasso and A. Nicolis, *Phys. Rev. D* **66**, 103505 (2002); C. Caprini and R. Durrer, *Phys. Rev. D* **74**, 063521 (2006); C. Caprini, R. Durrer and G. Servant, *Phys. Rev. D* **77**, 124015 (2008) [arXiv:0711.2593 [astro-ph]]; R. Aureda, M. Maggiore, A. Nicolis and A. Riotto, *Nucl. Phys. B* **631**, 342 (2002); A. Nicolis, *Class. Quant. Grav.* **21**, L27 (2004); C. Grojean and G. Servant, *Phys. Rev. D* **75**, 043507 (2007); S. J. Huber and T. Konstandin, arXiv:0806.1828 [hep-ph].
- [7] A. Megevand, *Phys. Rev. D* **78** (2008) 084003 [arXiv:0804.0391 [astro-ph]].

- [8] S. R. Coleman, Phys. Rev. D **15**, 2929 (1977) [Erratum-ibid. D **16**, 1248 (1977)]; C. G. Callan and S. R. Coleman, Phys. Rev. D **16**, 1762 (1977).
- [9] I. Affleck, Phys. Rev. Lett. **46**, 388 (1981); A. D. Linde, Nucl. Phys. B **216**, 421 (1983) [Erratum-ibid. B **223**, 544 (1983)]; Phys. Lett. B **100**, 37 (1981).
- [10] J. Ignatius, K. Kajantie, H. Kurki-Suonio and M. Laine, Phys. Rev. D **49**, 3854 (1994);
- [11] M. Dine, R. G. Leigh, P. Y. Huet, A. D. Linde and D. A. Linde, Phys. Rev. D **46**, 550 (1992) [arXiv:hep-ph/9203203].
- [12] B. H. Liu, L. D. McLerran and N. Turok, Phys. Rev. D **46**, 2668 (1992); N. Turok, Phys. Rev. Lett. **68**, 1803 (1992).
- [13] S. Y. Khlebnikov, Phys. Rev. D **46**, 3223 (1992); P. Arnold, Phys. Rev. D **48**, 1539 (1993) [arXiv:hep-ph/9302258].
- [14] G. D. Moore and T. Prokopec, Phys. Rev. D **52**, 7182 (1995) [arXiv:hep-ph/9506475]; Phys. Rev. Lett. **75**, 777 (1995) [arXiv:hep-ph/9503296].
- [15] G. D. Moore and N. Turok, Phys. Rev. D **55** 6538 (1997).
- [16] G. D. Moore, JHEP **0003**, 006 (2000);
- [17] P. John and M. G. Schmidt, Nucl. Phys. B **598**, 291 (2001) [Erratum-ibid. B **648**, 449 (2003)].
- [18] P. J. Steinhardt, Phys. Rev. D **25**, 2074 (1982).
- [19] M. Gyulassy, K. Kajantie, H. Kurki-Suonio and L. D. McLerran, Nucl. Phys. B **237** (1984) 477; T. DeGrand and K. Kajantie, Phys. Lett. B **147**, 273 (1984).
- [20] H. Kurki-Suonio, Nucl. Phys. B **255**, 231 (1985); K. Kajantie and H. Kurki-Suonio, Phys. Rev. D **34**, 1719 (1986).
- [21] K. Enqvist, J. Ignatius, K. Kajantie and K. Rummukainen, Phys. Rev. D **45**, 3415 (1992).
- [22] M. Laine, Phys. Rev. D **49**, 3847 (1994) [arXiv:hep-ph/9309242].
- [23] H. Kurki-Suonio and M. Laine, Phys. Rev. D **51**, 5431 (1995) [arXiv:hep-ph/9501216].
- [24] J. C. Miller and O. Pantano, Phys. Rev. D **40**, 1789 (1989); Phys. Rev. D **42**, 3334 (1990).
- [25] A. Megevand, Int. J. Mod. Phys. D **9**, 733 (2000) [arXiv:hep-ph/0006177]; Phys. Rev. D **64**, 027303 (2001) [arXiv:hep-ph/0011019]; Phys. Lett. B **642**, 287 (2006) [arXiv:astro-ph/0509291]; A. Bessa, E. S. Fraga and B. W. Mintz, arXiv:0811.4385 [hep-ph].

- [26] L. D. Landau and E. M. Lifshitz, *Fluid Mechanics* (Pergamon Press, New York, 1989); R. Courant and K. O. Friedrichs, *Supersonic Flow and Shock Waves* (Springer-Verlag, Berlin, 1985).
- [27] B. Link, Phys. Rev. Lett. **68**, 2425 (1992); K. Kajantie, Phys. Lett. B **285**, 331 (1992).
- [28] M. Kamionkowski and K. Freese, Phys. Rev. Lett. **69**, 2743 (1992) [arXiv:hep-ph/9208202].
- [29] P. Y. Huet, K. Kajantie, R. G. Leigh, B. H. Liu and L. D. McLerran, Phys. Rev. D **48**, 2477 (1993) [arXiv:hep-ph/9212224].
- [30] A. Megevand and A. D. Sánchez, Phys. Rev. D **77**, 063519 (2008) [arXiv:0712.1031 [hep-ph]].
- [31] M. Dine, P. Huet, R. L. . Singleton and L. Susskind, Phys. Lett. B **257**, 351 (1991).
- [32] M. Dine, P. Huet and R. L. . Singleton, Nucl. Phys. B **375**, 625 (1992).
- [33] G. W. Anderson and L. J. Hall, Phys. Rev. D **45**, 2685 (1992).
- [34] J. R. Espinosa and M. Quiros, Phys. Rev. D **76**, 076004 (2007) [arXiv:hep-ph/0701145]; J. R. Espinosa, T. Konstandin, J. M. No and M. Quiros, arXiv:0809.3215 [hep-ph]; A. Ashoorioon and T. Konstandin, arXiv:0904.0353 [hep-ph].
- [35] A. Mégevand and A. D. Sánchez, in preparation.
- [36] A. Megevand, Phys. Rev. D **69**, 103521 (2004).
- [37] D. Bodeker and G. D. Moore, arXiv:0903.4099 [hep-ph].
- [38] M. S. Carena, A. Megevand, M. Quiros and C. E. M. Wagner, Nucl. Phys. B **716**, 319 (2005) [arXiv:hep-ph/0410352].